Chemistry
A European
Journal

Chemistry Europe
European Chemical Societies Publishing

Accepted Article

Title: Structure-Activity Relationship Study of a Potent α-Thrombin Binding Aptamer Incorporating Hexitol Nucleotides

Authors: Maria De Fenza, Elena Eremeeva, Romualdo Troisi, Hui Yang, Anna Esposito, Filomena Sica, Piet Herdewijn, Daniele D'Alonzo, and Annalisa Guaragna

To be cited as: *Chem. Eur. J.* 10.1002/chem.202001504

Link to VoR: https://doi.org/10.1002/chem.202001504

WILEY-VCH

10.1002/chem.202001504

WILEY-VCH

FULL PAPER

Structure-Activity Relationship Study of a Potent α-Thrombin Binding Aptamer Incorporating Hexitol Nucleotides

Maria De Fenza,[a],† Elena Eremeeva,[b],† Romualdo Troisi,[a],† Hui Yang,[b] Anna Esposito,[a] Filomena Sica,[a] Piet Herdewijn,[b],* Daniele D'Alonzo[a],* and Annalisa Guaragna[a]

[a] Dr. M. De Fenza, R. Troisi, A. Esposito, Prof. Dr. F. Sica, Dr. D. D'Alonzo, Dr. A. Guaragna
Department of Chemical Sciences
Università degli Studi di Napoli Federico II
via Cintia, 80126 Napoli (Italy)
E-mail: dandalonzo@unina.it

[b] Dr. E. Eremeeva, H. Yang, Prof. Dr. P. Herdewijn
Rega Institute for Medical Research
Herestraat 49 - box 1041, 3000 Leuven (Belgium)
E-mail: piet.herdewijn@kuleuven.be

† Equal contribution

Supporting information for this article is given via a link at the end of the document.

Abstract: the replacement of one or more nucleotide residues in the potent α-thrombin-binding aptamer NU172 with hexitol-based nucleotides has been devised, studying the effect of these substitutions on the physicochemical and functional properties of the anticoagulant agent. The incorporation of single hexitol nucleotides at T9 and G18 positions of NU172 substantially retained the physicochemical features of the parent oligonucleotide, as a result of the biomimetic properties of the hexitol backbone. Importantly, the NU172-**T**^{H}9 mutant exhibited a higher binding affinity toward human α-thrombin than the native aptamer and an improved stability even after 24 h in 90% human serum, with a significant increase in the estimated half-life. The anticoagulant activity of the modified oligonucleotide was also found as slightly preferable than NU172. Overall, these results confirm the potential of hexitol nucleotides as biomimetic agents, while laying the foundations for the development of NU172-inspired α-thrombin-binding aptamers.

Introduction

Human α-thrombin is a serine protease playing opposite functional roles in blood coagulation.[1-3] α-Thrombin has procoagulant activity, as it causes blood clotting through proteolytic cleavage of fibrinogen and protease-activated receptors and activation of the essential clotting factors V, VIII, XI and XIII.[1,2] On the other hand, the same enzyme displays anticoagulant and antifibrinolytic activities when complexed with the transmembrane α-thrombin receptor thrombomodulin, owing to activation of the protein C and subsequent block of the coagulation cascade through the inactivation of the coagulation factors Va and VIIIa.[3-6]

α-Thrombin specificity is regulated by the presence of two anion-binding subsites, known as exosites I and II, which mediate binding to substrates, receptors, cofactors and inhibitors, thereby modulating the enzyme function.[7] Considering that an increased α-thrombin activity is associated with a variety of cardiovascular diseases,[8] the identification of anti-thrombin agents, selectively targeting α-thrombin sites, represents a successful strategy in anticoagulation therapy. In this area, anticoagulant oligonucletide aptamers are short, single-stranded DNA or RNA sequences that bind α-thrombin exploiting their ability to form elaborate three-dimensional structures.[9-12] They exhibit many favourable features for a perspective use as antithrombotic drugs or as α-thrombin biosensors, owing to the high affinity and specificity to the target, the low immunogenicity, as well as the low costs of production and the ease of chemical modification.[9-12] One of the earliest and most intensely investigated DNA-based α-thrombin inhibitors is represented by HD1 (also known as TBA), a DNA 15-mer (5'-GGTTGGTGTGGTTGG-3') inhibiting α-thrombin clotting activity at nanomolar concentration.[13] This oligonucleotide folds as a compact and symmetrical, chair-like, unimolecular antiparallel G-quadruplex structure, consisting of two G-tetrads connected by three edge-wise loops (T3-T4, T12-T13 and T7-G8-T9).[14] The aptamer tightly binds α-thrombin exosite I through the two TT loops, as revealed by the analysis of the complexes between α-thrombin and HD1 or its mutants.[15] Inspired by the success of HD1, a variety of novel, highly active DNA aptamers have been subsequently identified.[16-20] Among them, the DNA 26-mer NU172 (5'-CGCCTAGGTTGGGTAGGGTGGTGGCG-3') stands as one of the latest and most representative candidates in this field.[10] NU172 displayed one of the highest binding affinities toward human α-thrombin (K_D = 140 pM).[21,22] In contrast to other oligonucleotides, it was found to act as a fast-acting anticoagulant agent with no serious adverse effects.[10] NU172 is currently the only DNA aptamer reaching Phase II clinical trials for its use as anticoagulant agent in the treatment of heart diseases.[23]

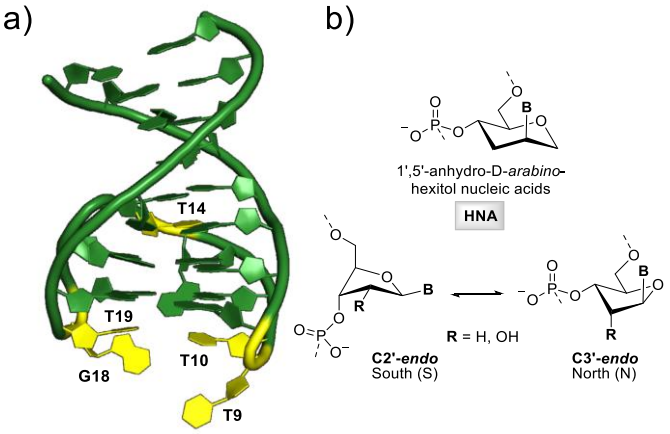

Figure 1. a) Crystallographic structure of NU172 when complexed with human α-thrombin (PDB ID: 6EVV). The residues modified throughout this work are highlighted in yellow. b) Hexitol nucleic acids (HNA) as sugar modified oligonucleotide analogues. The hexitol ring resembles the C3'-*endo* sugar ring pucker of native (deoxy)ribose in natural nucleotides.

10.1002/chem.202001504

From a structural standpoint, recent studies have revealed that NU172 adopts a mixed duplex/quadruplex architecture (Figure 1a) both in solution[24] and in the solid state when bound to α-thrombin.[25] The two antiparallel G-tetrads are connected by three key lateral loops (T9-T10, G18-T19 and G13-T14-A15), all driving the interaction with α-thrombin.[25] Despite the excellent binding affinity, target selectivity and anticoagulant activity, the short circulating *in vivo* half-life of HD1, NU172 and their congeners (e.g., HD1: $t_{1/2}$ ~1.8 min; NU172: $t_{1/2}$ ~10 min)[26,27] remains one of the most critical drawbacks hampering a potential development of nucleic acid aptamers as antithrombotic drugs.[9] Among the many strategies devised to overcome this long-standing limitation,[10,12] the chemical modification of the aptamer structure has been one of the most studied approaches,[28,29] involving changes in the sugar backbone,[30-37] the internucleotide linkages,[38-40] or sequence/length variations of key residues.[41-44] However, while modifications have been mainly focused on HD1,[30-34,36-44] no changes in the structure of NU172 have been reported so far. In this context, in the frame of a research program aimed to explore the biomimetic potential of various synthetic pairing systems,[45-49] we have focused attention on the analysis of the structural and functional changes in NU172 following the incorporation of unnatural nucleotides belonging to the class of Hexitol Nucleic Acids (HNA). HNA are sugar-modified nucleic acids, in which native ribonucleotides are replaced by 1',5'-anhydro-D-*arabino*-hexitol nucleotides (Figure 1b). The HNA system represents one of the most prominent examples of conformationally constrained oligonucleotide analogues.[50,51] HNA has demonstrated to act as an A-type (RNA) mimic, since the $^4C_1$ sugar conformation of the hexitol ring resembles the bioactive C3'-*endo* (*North*) sugar ring pucker of natural (deoxy)ribonucleotides.[51,52] The six-membered hexitol moiety makes HNA a preorganized oligonucleotide construct toward complex formation, resulting in a sequence-dependent enhancement of the thermodynamic stability of both duplexes[53] and quadruplexes[54] when compared to unmodified complexes. In addition, HNA exhibited high stability against nucleases.[55] Over the years, the utility of HNA as biomimetic oligonucleotides has been demonstrated in a variety of applications, ranging from medicinal chemistry[55,56] to synthetic biology,[57-59] and the impact of HNA in aptamer research has been already recognized.[57,60,61] The involvement of HNA in the development of α-thrombin-binding aptamers takes place from the conformational analysis of NU172 nucleotides, as resulting from the crystal structure of the aptamer in complex with human α-thrombin.[25] Differently from HD1, in which all nucleotides are reported to adopt *South* conformations,[29] two key nucleotides of NU172, both engaged in α-thrombin binding, were found to have different conformational preferences. Particularly, deoxyguanosine at position 18 (G18) adopted a pure C3'-*endo* sugar ring pucker, presumably as a consequence of a hydrogen bonding with G13;[25] on the other hand, the thymidine residue at position 9 (T9) was arranged in a O4'-*endo* sugar conformation, which is intermediate between *North* and *South* forms. Based on these observations, this work is primarily focused on the incorporation of hexitol nucleotides into these positions, to study whether a beneficial effect on binding affinity and/or nuclease stability could be gained from the insertion of these highly preorganized and stable nucleotide analogues. Crucial positions T10, T14 and T19 were also modified, because of their involvement in the interaction with α-thrombin[25] or in nuclease digestion.[62,63]

Materials and Methods

Chemistry

Nucleoside Synthesis: hexitol thymidine and guanosine nucleosides were synthesized as described previously[64] (see ESI for further details). All moisture-sensitive reactions were performed under a nitrogen atmosphere using oven-dried glassware. Solvents were dried over standard drying agents and freshly distilled prior to use. All chemicals were purchased from VWR or Merck Life Science at their highest degree of purity available. Reactions were monitored by TLC (pre coated silica gel plate F254, Merck). TLC visualization methods: UV exposure. TLC stains: I_2, ninhydrin, sulfuric acid. Column chromatography: Merck Kieselgel 60 (70-230 mesh). ^1H and ^{13}C NMR spectra were recorded on NMR spectrometers operating on Bruker DRX (400 MHz), Varian Inova Marker (500 MHz) or Varian (600 MHz) using $CDCl_3$ solutions unless otherwise specified.

Oligonucleotide Synthesis: oligonucleotide assembly was performed with an Expedite DNA synthesizer (Applied Biosystems) by using the phosphoramidite approach. The oligonucleotides were deprotected and cleaved from the solid support by treatment with aqueous ammonia (33%) for 2 h at 55°C. After gel filtration on a NAP-25 column (Sephadex G25-DNA grade) with water as eluent, the crude mixtures were analyzed by using a Mono-Q HR 5/5 anion exchange column, after which purification was achieved by using a Mono-Q HR 10/100 GL column (Pharmacia) with the following gradient system: Buffer A: 10 mM NaOH in 0.1 M NaCl, pH 12.0 and Buffer B: 10 mM NaOH in 0.9 M NaCl, pH 12.0. After gel filtration, oligonucleotides were re-purified with the following gradient system: Buffer A: 0.1 M triethylammonium acetate (TEAA) with 5% CH_3CN, pH 7.5 and Buffer B: 0.1 M TEAA with 80% CH_3CN, pH 7.5. The low-pressure liquid chromatography system consisted of a HITACHI Primaide organizer with a HITACHI Primaide 1410 UV detector and with a HITACHI Primaide 1110 pump and a Mono-Q HR 10/100 GL column (Pharmacia). The product-containing fractions were desalted on a NAP-25 column and lyophilized. Analysis by mass spectrometry was performed (see ESI). All oligonucleotides (Table 1) were first folded in the SB buffer (Table S3) by heating to 95°C for 5 min followed by slow cooling to 8°C and equilibration to room temperature.

Spectroscopic Analysis

Sample preparation: oligonucleotides were suspended in 10 mM potassium phosphate buffer pH 7.4 and 100 mM KCl at a concentration ranging between 10 μM (CD experiments) and 20 μM (UV experiments). In order to induce folding, all oligonucleotide samples were annealed by heating to 90°C for 5 minutes and then slow cooling down in 50-60 minutes and storing at 20°C overnight.

Circular dichroism measurements: the spectra were recorded at 10°C using a Jasco J-715 spectropolarimeter equipped with a Peltier temperature control. CD measurements were carried out in the 220–320 nm range, using a 0.1 cm path length cell. Thermal unfolding curves were obtained by following the CD signal at 295 nm and by recording 220–320 nm spectra in 2°C steps with 5 s equilibration time between readings, in the 10–90°C range, at heating rate 1.0°C min^{-1}. The fraction of folded oligonucleotide was calculated as [$F_{folded} = (I_{obs} - I_u)/(I_f - I_u)$], where I_{obs} is the CD signal at 295 nm at each temperature, I_f and I_u are the CD signals at 295 nm for the folded (at T = 10°C) and unfolded (at T = 90°C) oligonucleotide, respectively. The melting temperatures were

obtained through analysis of the first derivative of the melting profiles. Moreover, when possible, melting temperatures, as well as thermodynamic parameters of the unfolding process, were also derived from van't Hoff analysis of melting profiles.[65]

UV experiments: UV melting profiles were recorded using an Agilent Technology Cary Series 100 UV-Vis spectrophotometer equipped with a Peltier thermostatic cell holder. Thermal unfolding was monitored in the 10–90°C range at two different wavelengths, 260 and 297 nm, using a 0.1 cm and 0.5 cm path-length quartz micro-cuvette, respectively. The heating rate was 1°C min^{-1}. UV melting profiles at both 260 nm and 297 nm were reported as normalized ΔA (NΔA) as a function of temperature. Normalized ΔA was calculated as [$N\Delta A = (A_{obs} - A_{min})/(A_{max} - A_{min})$] where A_{obs} is the UV absorbance at 260 or 297 nm at each temperature, A_{max} and A_{min} are the highest and the lowest absorbance recorded in the melting experiment, respectively. Melting temperatures were obtained through analysis of the first derivative of the melting profiles. Van't Hoff analysis[65] was carried out when possible.

α-Thrombin-binding Properties and Nuclease Stability

Materials: human α-Thrombin native protein, whole human serum and SYBR Gold Nucleic Acid Gel Stain (10000×) were purchased from ThermoFisher scientific. Low Molecular Weight DNA Ladder was obtained from New England Biolabs. All other chemicals were obtained either from VWR or Sigma-Aldrich.

Electrophoretic mobility shift assay (EMSA): 50 µL of the total reaction volume containing 200 nM of renatured oligonucleotide solutions without or with 200 nM of human α-thrombin in SB was incubated for 2 h at room temperature (rt) upon shaking at 300 rpm. After incubation, 10 µL of 6× gel loading buffer was added to the samples, and 20 µL of the final solutions was run on a 6% Native PAGE (see Table S3 for details) with 0.5× TBE (running buffer) at 150 V and ~ 18 °C until the bromophenol blue dye was ~ 3 cm below the bottom of the gel wells (~ 1.5 h). Gels were first incubated in 1× SYBR Gold Nucleic Acid Gel Stain for 10 min. All samples were scanned using the Typhoon 9500 imaging system (Cy2-channel) and quantified with the ImageQuant TL v8.1 software (both from GE Healthcare Life Science). Band intensities of each oligonucleotide variant were measured as intensity volumes in a lane, normalized by that of unmodified NU172 aptamer (taken as 100%), and the relative binding abilities were calculated. Mean values with standard deviation from three independent experiments were plotted to the graph.

Stability in human serum: unmodified and HNA-modified oligonucleotide variants (1 or 2 µM each) were incubated in 90% whole human serum at 37°C in 100 µL total reaction volume. Aliquots (10 µL) of each reaction were taken at different time intervals (0, 1, 6, 24, 48, and 72 h). Then 10 µL of H_2O was added to each aliquot together with 20 µL of 2× quenching buffer (see Table S3 for buffer composition). The samples were denatured at 95°C for 10 min, then were kept at -20°C until analysis by denaturing 15% PAGE (see Table S3 for details). Gels were incubated in 1× SYBR Gold Nucleic Acid Gel Stain for 10 min and visualized using the Typhoon 9500 imaging system (Cy2-channel) and the ImageQuant TL v8.1 software. The analysis was performed in duplicate and average band intensities corresponding to the full-size oligonucleotide in each time point (normalized by that at 0 h point) were plotted on the graph. The half-life values were calculated as the time required for 50% degradation of the original intact aptamer.

Table 1. Sequences of NU172 and its mutants.

Entry	Name	Sequence, 5'→3'
1	NU172	d(CGCCTAGGTTGGGTAGGGTGGTGGCG)
2	NU172-**T**^{H}9	d(CGCCTAGG**T**^{H}TGGGTAGGGTGGTGGCG)
3	NU172-**T**^{H}10	d(CGCCTAGGT**T**^{H}GGGTAGGGTGGTGGCG)
4	NU172-**T**^{H}14	d(CGCCTAGGTTGGG**T**^{H}AGGGTGGTGGCG)
5	NU172-**G**^{H}18	d(CGCCTAGGTTGGGTAGG**G**^{H}TGGTGGCG)
6	NU172-**T**^{H}19	d(CGCCTAGGTTGGGTAGGG**T**^{H}GGTGGCG)
7	NU172-**T**^{H}9**T**^{H}14	d(CGCCTAGG**T**^{H}TGGG**T**^{H}AGGGTGGTGGCG)
8	NU172-**T**^{H}9**G**^{H}18	d(CGCCTAGG**T**^{H}TGGGTAGG**G**^{H}TGGTGGCG)
9	NU172-**T**^{H}9**T**^{H}19	d(CGCCTAGG**T**^{H}TGGGTAGGG**T**^{H}GGTGGCG)
10	NU172-**G**^{H}18**T**^{H}19	d(CGCCTAGGTTGGGTAGG**G**^{H}**T**^{H}GGTGGCG)
11	NU172-**T**^{H}9**T**^{H}14**G**^{H}18	d(CGCCTAGG**T**^{H}TGGG**T**^{H}AGG**G**^{H}TGGTGGCG)
12	NU172-**T**^{H}9**G**^{H}18**T**^{H}19	d(CGCCTAGG**T**^{H}TGGGTAGG**G**^{H}**T**^{H}GGTGGCG)
13	NU172-**T**^{H}9**T**^{H}10**G**^{H}18**T**^{H}19	d(CGCCTAGG**T**^{H}**T**^{H}GGGTAGG**G**^{H}**T**^{H}GGTGGCG)

N^{H} represents the modified hexitol nucleotide.

Anticoagulant Activity

Sample preparation: human α-thrombin and fibrinogen from human plasma were purchased from Haematologic Technologies (USA) and Sigma-Aldrich (United Kingdom), respectively. Oligonucleotides were suspended in 10 mM potassium phosphate buffer pH 7.4 and 100 mM KCl at a concentration of 10 μM. In order to induce folding, all oligonucleotide samples were annealed by heating to 90°C for 5 minutes and then slow cooling down in 50-60 minutes and storing at 20°C overnight.

Anticoagulant activity experiments: the α-thrombin-induced clotting of fibrinogen was measured spectrophotometrically.[66] A 1.8 mg mL^{-1} solution of fibrinogen in Phosphate Buffered Saline (PBS) was placed in a PS cuvette to which the oligonucleotide was added and left to equilibrate in the instrument for 5 min. Then, α-thrombin was added up to a final concentration of 5 nM. The time required for fibrin polymerization was determined from a UV scattering curve (380 nm), recorded over time in the presence of each oligonucleotide. Each curve was determined in triplicate at different oligonucleotide concentrations (20, 40, and 80 nM). Clotting time was derived from the maximum of the second derivative of each scattering curve. The basal clotting time was determined in the absence of oligonucleotide (9 s). Fibrinogen clotting times of NU172 and its variants were calculated by subtracting the basal clotting time.

Results

Chemistry

Hexitol thymidine and guanosine nucleosides were synthesized as described previously,[64] with some changes in the original synthetic route leading to an enhancement of the overall yield regarding the preparation of the guanosine monomer (see ESI for full details). Oligonucleotide sequences containing single or multiple incorporations of hexitol nucleotides **T**^{H} and **G**^{H} (Table 1) were prepared with a DNA synthesizer by using the phosphoramidite approach.

Spectroscopic analysis

In order to evaluate the effect of hexitol nucleotides on structure and thermal stability of the corresponding NU172 aptamer, a spectroscopic analysis of the modified oligonucleotides was performed. In first studies, the biomimetic potential of HNA was explored by CD analysis (Figure 2). As previously reported,[22] the CD spectrum of NU172 in the presence of potassium ions (Figures 2a-c, black line) displayed two positive signals at 245 and 295 nm and one negative signal at 265 nm, which are distinctive of the antiparallel G-quadruplex architecture.[67] Accordingly, changes in the profile or in the intensity of CD spectra were analysed for each mutant with respect to the unmodified aptamer (Figures 2a-c and Figure S1). Single incorporations were first considered (Figure 2a). The T14→**T**^{H}14 mutation had a detrimental effect on the conformational integrity of the oligonucleotide, as estimated by the reduced intensity of the signals at 245, 265 and 295 nm. The modified oligonucleotide carrying the **T**^{H}10 nucleotide displayed a fully different CD spectrum compared to NU172, as it exhibited two positive bands at 265 and 295 nm, suggesting a conformational heterogeneity. Conversely, the NU172-**G**^{H}18 and NU172-**T**^{H}19 mutants exhibited a CD profile substantially superimposable to that of the native aptamer, strongly indicating that the presence of the unnatural deoxyguanosine and thymidine at these positions did not produce differences in the conformational behaviour of NU172. Furthermore, CD spectrum of NU172-**T**^{H}9 mutant displayed an enhancement in the intensity of all bands, indicating a more compact folding of this oligonucleotide. In particular, the increase in the intensity of the CD signal at 295 nm suggests a more pronounced propensity than NU172 to adopt an antiparallel G-quadruplex structure.

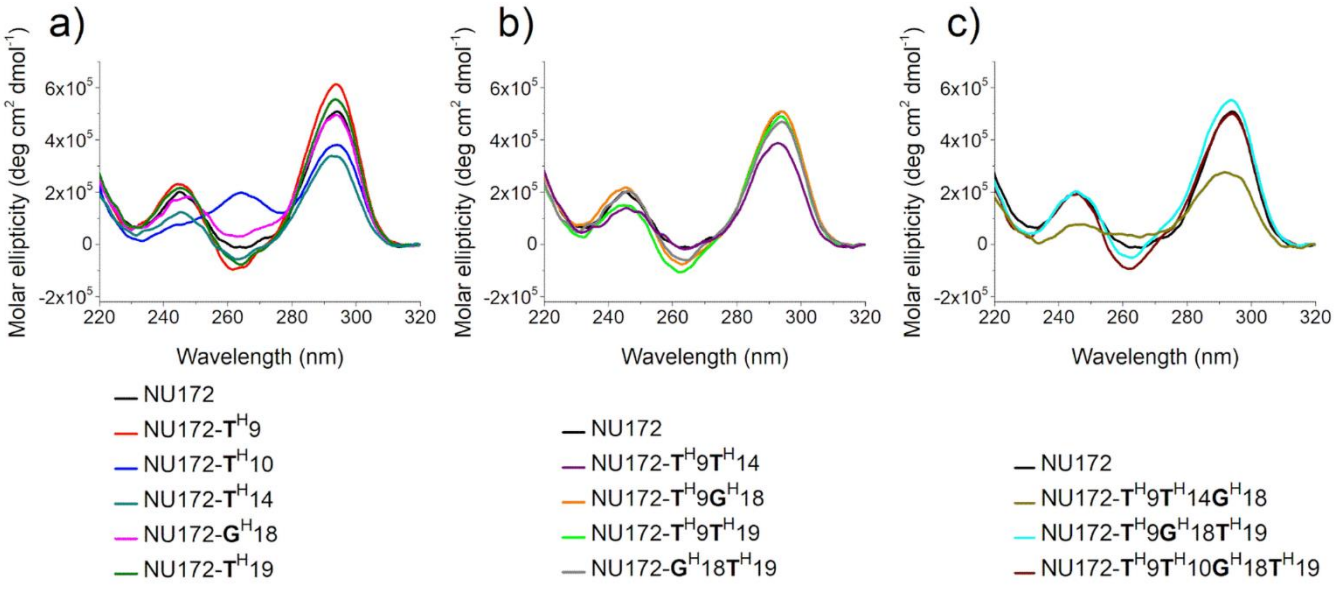

Figure 2. CD spectra of NU172 and its variants containing a) one mutation, b) two mutations, c) three or four mutations. Spectra were recorded at 10°C on oligonucleotide samples (10 μM) previously annealed in 10 mM potassium phosphate buffer pH 7.4 and 100 mM KCl.

10.1002/chem.202001504

Multiple incorporations were also considered (Figures 2b-c). In line with data on single incorporations, the presence of **T**^{H}14 in NU172-**T**^{H}9**T**^{H}14 and NU172-**T**^{H}9**T**^{H}14**G**^{H}18 mutants significantly destabilized the structure of the oligonucleotides. On the other hand, the mutants carrying the **T**^{H}9**G**^{H}18, **T**^{H}9**T**^{H}19, **G**^{H}18**T**^{H}19, **T**^{H}9**G**^{H}18**T**^{H}19 or **T**^{H}9**T**^{H}10**G**^{H}18**T**^{H}19 nucleotides displayed broadly unchanged intensities of the CD signals compared to NU172.

CD analysis was also conducted to provide indications on the thermal stability of the modified oligonucleotides, plotting the fraction of folded oligonucleotides as a function of temperature (Figure S2). Melting temperature (T_m) values (Table 2) obtained for most NU172 mutants were lower than that reported for the native aptamer, indicating that the hexitol incorporations perturb the thermal stability of NU172. Conversely, oligonucleotides carrying mutations **T**^{H}9, **G**^{H}18, and **T**^{H}9**G**^{H}18 (entries 2, 5 and 8) essentially retained the thermal temperature of the unmodified aptamer. Except for NU172-**T**^{H}10, the superimposition of CD spectra obtained during denaturation experiments provided isodichroic points at about 253 and 279 nm (Figures S3-S5), which is an indication of a two-state unfolding process. Moreover, the reversibility of the thermal unfolding process of all samples was confirmed by the full recovery of spectral features after cooling to 10°C upon heat denaturation. Within the limits of experimental errors, the $\Delta H_{v.H}$ and $\Delta S_{v.H}$ values obtained by the van't Hoff analysis of the melting curves (Table S1) together with the CD spectra clearly suggest that the insertion of the hexitol moiety in T9 or G18 does not impair a full acquisition of a quadruplex organization similar to NU172.

Table 2. Melting temperatures of NU172 and its variants obtained by temperature-dependent CD and UV measurements.

Entry	Oligonucleotide	T_m (°C) (CD at 295 nm)[a]	T_m (°C) (UV at 297 nm)[a]	T_m (°C) (UV at 260 nm)[a]
1	NU172	47	48	52
2	NU172-**T**^{H}9	48	49	53
3	NU172-**T**^{H}10	ND[b]	47	ND[b]
4	NU172-**T**^{H}14	41	43	ND[b]
5	NU172-**G**^{H}18	48	49	52
6	NU172-**T**^{H}19	44	45	52
7	NU172-**T**^{H}9**T**^{H}14	43	ND	ND
8	NU172-**T**^{H}9**G**^{H}18	48	ND	ND
9	NU172-**T**^{H}9**T**^{H}19	44	ND	ND
10	NU172-**G**^{H}18**T**^{H}19	45	ND	ND
11	NU172-**T**^{H}9**T**^{H}14**G**^{H}18	42	ND	ND
12	NU172-**T**^{H}9**G**^{H}18**T**^{H}19	46	ND	ND
13	NU172-**T**^{H}9**T**^{H}10**G**^{H}18**T**^{H}19	42	ND	ND

ND: not determined.

[a] Temperatures were calculated as the average of two independent measurements: errors range between 0.5 and 1.0 °C.

[b] The melting curve trends hamper a correct determination of T_m value.

10.1002/chem.202001504

The effect of the incorporation of a single hexitol nucleotide on the chemical stability of NU172 was also investigated by temperature-dependent UV studies. The X-ray analysis of NU172 revealed the concurrent existence of quadruplex and duplex domains, the latter relying on W-C base pairs C1:G26, G2:C25, C3:G24 and C4:G23.[25] Accordingly, the stability of both duplex and quadruplex complexes in the modified oligonucleotides was evaluated by studying their absorbance variation at 260 and 297 nm, respectively (Table 2 and Figure S6). Indeed, at 297 nm a hypochromic shift with increasing temperature is associated with G-quadruplex melting.[68,69] In contrast, a double helix DNA experiences a hyperchromic shift at 260 nm upon increasing temperature.[24,70] Single incorporations of hexitol nucleotides generally led to slight to marked reductions (Table 2, entries 3, 4 and 6) in the stability of the oligonucleotides. As exceptions, modifications at positions T9 (NU172-**T**^{H}9, entry 2) and G18 (NU172-**G**^{H}18, entry 5) did not perturb the stability of both the quadruplex and the duplex of the native aptamer (entry 1). $\Delta H_{v.H}$ and $\Delta S_{v.H}$ values from UV melting curves (Table S2) show the same trend shown by CD data.

α-Thrombin-binding properties

The binding affinity of the oligonucleotides toward human α-thrombin was carried out by Electrophoretic Mobility Shift Assay (EMSA) (Figure 3). Compared with the unmodified aptamer (Figure 3b, lane 1), the relative binding affinity of NU172-**T**^{H}9 was enhanced to 23% (lane 2). On the other hand, the affinities of the oligonucleotides bearing mutations **G**^{H}18 and **T**^{H}19 (lanes 4 and 5) were almost equivalent (96-102%) to that of native NU172. Detrimental was the substitution T10 → **T**^{H}10, leading to a reduced binding ability (57%, lane 3). Replacement of the native sequence with four hexitol nucleotides (lane 6) led to an almost complete loss of the binding ability to α-thrombin (5%; Figure 3).

Nuclease stability

The stability of selected oligonucleotides against nuclease digestion was then examined, as resulting from the incubation of the oligonucleotides with 90% human serum at 37°C (Figures 4 and S7). Oligonucleotides bearing mutations **T**^{H}10, **T**^{H}19 and **T**^{H}9**T**^{H}10**G**^{H}18**T**^{H}19 exhibited lower stability than NU172 upon 72 h of incubation. The estimated half-life values for these oligonucleotides suggested that only in the case of NU172-**T**^{H}19 (13.3 h) this time was comparable to that of NU172 (12.3 h), while as expected $t_{1/2}$ values were significantly lower for the remaining oligonucleotides (NU172-**T**^{H}10: 4.7 h; NU172-**T**^{H}9**T**^{H}10**G**^{H}18**T**^{H}19: 5.6 h). The NU172-**G**^{H}18 mutant displayed a slightly higher stability than the unmodified aptamer, with a maximum enhancement at 48 h, which was however rather limited (1.6-fold). In this case, half-life estimation indicated an increase in the $t_{1/2}$ value up to 17.0 h. On the other hand, we found a remarkable effect by NU172-**T**^{H}9, whose integrity was substantially unaffected after 6 h of incubation (92%). Under the same conditions, the stability of the unmodified NU172 decreased to 60%. The NU172-**T**^{H}9 mutant exhibited a significantly improved stability even after 24 h (1.7-fold increase), and only after 48 h of incubation the stability of NU172-**T**^{H}9 and NU172 was roughly the same (NU172-**T**^{H}9: 28%; NU172: 21%; Figure 4). Remarkably, overall the half-life value of NU172-**T**^{H}9 resulted over 2-fold higher (28.6 h) than that of the unmodified oligonucleotide. Other selected mutants displayed only reduced stability compared to NU172 and NU172-**T**^{H}9 upon 24 h of incubation (Figure S8).

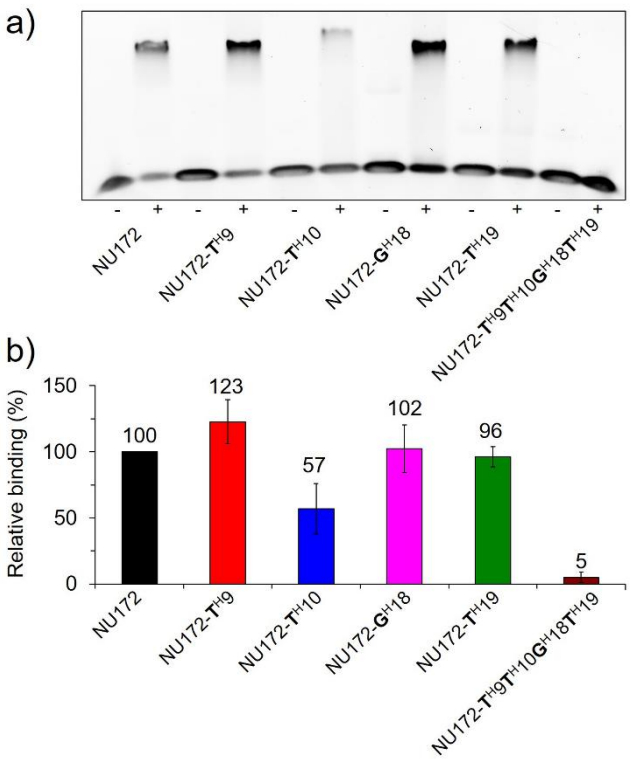

Figure 3. Evaluation of the binding affinity of anti-thrombin NU172 variants by EMSA. a) Oligonucleotides (200 nM) were incubated without ('-' samples) or with ('+' samples) human α-thrombin (200 nM) at 37°C for 2 h. Oligonucleotide-α-thrombin complexes were separated from free oligonucleotides on a 6% Native PAGE. b) The relative binding abilities compared to the unmodified aptamer (taken as 100%) were calculated from three independent experiments.

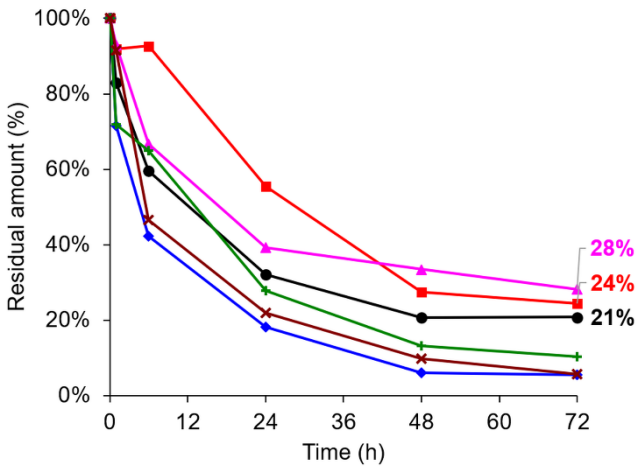

Figure 4. Stability in human serum of NU172 (●) and its mutants bearing **T**^{H}9 (■), **T**^{H}10 (♦), **G**^{H}18 (▲), **T**^{H}19 (+) or **T**^{H}9**T**^{H}10**G**^{H}18**T**^{H}19 (x) nucleotides. Oligonucleotides (2 μM) were incubated in 90% human serum at 37°C for up to 72 h.

Anticoagulant activity

The ability by NU172 variants to compete with fibrinogen for α-thrombin exosite I was eventually evaluated, performing a spectrophotometrical fibrinogen clotting assay[66] (Figure 5). Modifications at T10 and T19 of NU172 had a detrimental effect on the anticoagulant activity, leading to a significant decrease of the clotting times compared to the unmodified aptamer over the explored concentration range (20-80 nM). In the case of NU172-

10.1002/chem.202001504

G^{H}18 mutant, the clotting time was slightly longer than previous oligonucleotides, although its anticoagulant activity was much lower than NU172. On the other hand, NU172-**T**^{H}9 retained the anticoagulant activity of NU172 at low dosage, while this was slightly enhanced at high concentrations, with a 1.2-fold increase at 80 nM (Figure 5).

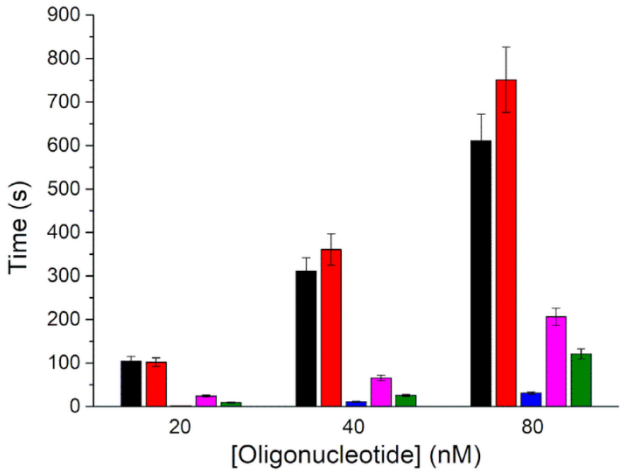

Figure 5. Prolonged fibrinogen clotting times measured in PBS buffer in the presence of fibrinogen (1.8 mg/mL), α-thrombin (5 nM), and either NU172 (black) or oligonucleotides carrying mutations **T**^{H}9 (red), **T**^{H}10 (blue), **G**^{H}18 (magenta) and **T**^{H}19 (green) at concentrations of 20, 40 and 80 nM.

Discussion

The focus of this work is the analysis of the physicochemical and functional properties of anticoagulant oligonucleotides deriving from the incorporation of hexitol nucleotides into specific positions of the highly active α-thrombin-binding aptamer NU172. Following the identification of three nuclease-sensitive side loops T9-T10, G18-T19, and G13-T14-A15 as key sequences involved in the α-thrombin-binding process,[25] single and multiple incorporations of **T**^{H} and **G**^{H} nucleotides were conceived at these positions of NU172, in order to study the capacity by the rigid six-membered nucleotides to improve nuclease resistance and to enhance the binding properties of the resulting modified oligonucleotides. Accordingly, the spectroscopic analysis of NU172 mutants well correlates the conformational preferences of native nucleotides in NU172 with the biomimetic properties of hexitol nucleotides. The NU172-**G**^{H}18 mutant keeps the structural properties of the parent aptamer, as expected owing to the ability by $^{4}C_{1}$ sugar chair in G18 to faithfully resemble the C3'-*endo* conformation adopted by the same nucleotide in the parent aptamer. Conversely, the incorporation of hexitol nucleotides at positions T10, T14, and T19 negatively affects the conformational properties and/or the thermal stability of the corresponding oligonucleotides. This can be easily rationalized, since these nucleotide residues adopt a C2'-*endo* sugar puckering in the unmodified aptamer. The highly destabilizing effect is especially apparent for NU172-**T**^{H}14, considering that in NU172 the T14 residue is involved in a tight junction between duplex and quadruplex domains.[25] Concerning the NU172-**T**^{H}9 mutant, the aptitude of the hexitol nucleotide to not interfere with the structural and thermal proprieties of NU172 suggests that the hexitol moiety can be properly accommodated into the oligonucleotide, despite the fact that the modified nucleotide does not closely reproduce the O4'-*endo* form of T9 in NU172. The spectral features of NU172-**T**^{H}9**G**^{H}18, which are superimposable to those of the unmodified aptamer, also suggest that both modified nucleotides do not perturb the integrity of the duplex/quadruplex architecture of NU172.

The binding affinity towards α-thrombin of the modified oligonucleotides was consistent with their-biological stability. The NU172-**T**^{H}9 mutant was the best binder to human α-thrombin in EMSA studies, while the binding affinity of the **G**^{H}18-containing oligonucleotide was unchanged with respect to NU172. The tightest binders NU172-**T**^{H}9 and NU172-**G**^{H}18 as observed by EMSA also displayed the highest resistance to nuclease hydrolysis.

Eventually, clotting time experiments show that NU172-**T**^{H}9 is the only oligonucleotide with comparable or slightly enhanced anticoagulant activity than the unmodified NU172.

Conclusions

We have herein compiled the first report on the synthesis, the structural characterization, the evaluation of the α-thrombin-binding properties and the anticoagulation activity of NU172 analogues, obtained by incorporation of unnatural hexitol-based nucleotides into key positions of the aptamer. Spectroscopic analysis has revealed that modifications at T9 or G18 positions leave almost unchanged both structure and thermal stability of NU172. In contrast, substitutions at T10, T14 and T19 positions negatively affect the structural proprieties of the parent aptamer.

In particular, based on this structure-activity relationship study, we identified in NU172-**T**^{H}9 the most interesting NU172 analogue. It exhibited a higher binding affinity toward human α-thrombin than the native oligonucleotide (23% increase). In addition, **T**^{H}9 incorporation produced a significant enhancement in the estimated half-life of NU172 in 90% human serum. The anticoagulant activity of NU172-**T**^{H}9, evaluated through a fibrinogen clotting assay, was also found as comparable or slightly preferable than the unmodified oligonucleotide. Overall, this study confirms the potential of HNA as biomimetic agent, and more generally highlights the role of sugar preorganization affecting binding affinity, half-life and clot formation of the corresponding NU172-derived modified oligonucleotides. Starting from this first candidate, more extensive modifications will help to find optimal binders and anticoagulant agents among hexitol-based oligonucleotides.

Acknowledgements

We thank Prof. Emanuele De Vendittis (Department of Molecular Medicine and Medical Biotechnology, University of Naples Federico II, Naples, Italy) for permission to use the Agilent Technology Cary Series 100 UV-Vis instrument. Authors are indebted to Prof. Jef Rozenski for mass spectrometry analysis and Guy Schepers for the chemical synthesis of oligonucleotides. E. E. acknowledges the Fonds Wetenschappelijk Onderzoek (FWO, Flanders Research Foundation) for funding (grant number 12Q8619N).

Keywords: anticoagulant activity • duplex/quadruplex aptamers • hexitol nucleic acids • human α-thrombin inhibitors • NU172.

References

[1] E. Di Cera, *J. Thromb. Haemost.* **2007**, *5*, 196–202.

[2] E. Di Cera, *Mol. Aspects Med.* **2008**, *29*, 203–254.

[3] E. Di Cera, Q. D. Dang, Y. M. Ayala, *Cell. Mol. Life Sci. CMLS* **1997**, *53*, 701–730.

[4] P. Fuentes-Prior, Y. Iwanaga, R. Huber, R. Pagila, G. Rumennik, M. Seto, J. Morser, D. R. Light, W. Bode, *Nature* **2000**, *404*, 518–525.

[5] C. T. Esmon, *FASEB J.* **1995,** *9*,946-55.

[6] B. Dahlbäck, B. O. Villoutreix, *Arterioscler Thromb Vasc Biol.* **2005**, *25*, 1311–1320.

[7] J. T. B. Crawley, S. Zanardelli, C. K. N. K. Chion, D. A. Lane, *J. Thromb. Haemost.* **2007**, *5*, 95–101.

[8] S. Danckwardt, M. W. Hentze, A. E. Kulozik, *J. Mol. Med.* **2013**, *91*, 1257–1271.

[9] A. D. Keefe, S. Pai, A. Ellington, *Nat. Rev. Drug Discov.* **2010**, *9*, 537–550.

[10] J. Zhou, J. Rossi, *Nat. Rev. Drug Discov.* **2017**, *16*, 181–202.

[11] S. M. Nimjee, R. R. White, R. C. Becker, B. A. Sullenger, *Annu. Rev. Pharmacol. Toxicol.* **2017**, *57*, 61–79.

[12] S. I. Ismail, W. Alshaer, *Adv. Drug Deliv. Rev.* **2018**, *134*, 51–64.

[13] L. C. Bock, L. C. Griffin, J. A. Latham, E. H. Vermaas, J. J. Toole, *Nature* **1992**, *355*, 564–566.

[14] R. F. Macaya, P. Schultze, F. W. Smith, J. A. Roe, J. Feigon, *Proc. Natl. Acad. Sci.* **1993**, *90*, 3745–3749.

[15] a) I. Russo Krauss, A. Merlino, C. Giancola, A. Randazzo, L. Mazzarella, F. Sica, *Nucleic Acids Res.* **2011**, *39*, 7858–7867; b) I. Russo Krauss , A. Merlino, A. Randazzo, E. Novellino, L. Mazzarella, F. Sica, *Nucleic Acids Res.* **2012**, *40*, 8119-8128; c) I. Russo Krauss, V. Spiridonova, A. Pica, V. Napolitano, F. Sica, *Nucleic Acids Res.* **2016**, *44*, 983-991.

[16] D. M. Tasset, M. F. Kubik, W. Steiner, *J. Mol. Biol.* **1997**, *272*, 688–698.

[17] C. P. Rusconi, E. Scardino, J. Layzer, G. A. Pitoc, T. L. Ortel, D. Monroe, B. A. Sullenger, *Nature* **2002**, *419*, 90–94.

[18] K. Ikebukuro, Y. Okumura, K. Sumikura, I. Karube, *Nucleic Acids Res.* **2005**, *33*, e108–e108.

[19] E. Y. Savchik, T. B. Kalinina, N. N. Drozd, V. A. Makarov, E. G. Zav'yalova, E. N. Lapsheva, N. N. Mudrik, A. V. Babij, G. V. Pavlova, A. V. Golovin, A. M. Kopylov, *Bull. Exp. Biol. Med.* **2013**, *156*, 44–48.

[20] K. Wakui, T. Yoshitomi, A. Yamaguchi, M. Tsuchida, S. Saito, M. Shibukawa, H. Furusho, K. Yoshimoto, *Mol. Ther. - Nucleic Acids* **2019**, *16*, 348–359.

[21] J. L. Diener, J. Wagner-Whyte, D. Fontana, US7998939B2, **2011**.

[22] E. Zavyalova, N. Ustinov, A. Golovin, G. Pavlova, A. Kopylov, *Curr. Med. Chem.* **2016**, *23*, 1-15.

[23] Study of NU172 as Anticoagulation in Patients Undergoing Off-pump CABG Surgery. https://clinicaltrials.gov/ct2/show/NCT00808964 (accessed Feb 16, 2020).

[24] I. Russo Krauss, V. Napolitano, L. Petraccone, R. Troisi, V. Spiridonova, C. A. Mattia, F. Sica, *Int. J. Biol. Macromol.* **2018**, *107*, 1697–1705.

[25] R. Troisi, V. Napolitano, V. Spiridonova, I. Russo Krauss, F. Sica, *Nucleic Acids Res.* **2018**, *46*, 12177–12185.

[26] W.A. Lee, J.A. Fishback, J. P. Shaw, L. C. Bock, L. C. Griffin, K. C. Cundy, *Pharm. Res.* **1995**, *12*, 1943-1947.

[27] R. De Caterina, S. Husted, L. Wallentin, F. Andreotti, H. Arnesen, F. Bachmann, C. Baigent, K. Huber, J. Jespersen, S. D. Kristensen, G. Y. H. Lip, J. Morais, L. H. Rasmussen, A. Siegbahn, F. W. A. Verheugt, J. I. Weitz, *Thromb Haemost* **2013**; *109*, 569-579.

[28] R. E. Wang, H. Wu, Y. Niu, J. Cai, *Curr. Med. Chem.* **2011**, 18, 4126-4138.

[29] a) A. Avino, C. Fabrega, M. Tintore, R. Eritja, *Curr. Pharm. Des.* **2012**, 18, 2036-2047; b) A. Aviñó, S. Mazzini, R. Ferreira, R. Gargallo, V. E. Marquez, R. Eritja *Bioorg. Med. Chem.* **2012**, *20*, 4186-4193; c) H. Saneyoshi, S. Mazzini, A. Avino, G. Portella, C. Gonzalez, M. Orozco, V. E. Marquez, R. Eritja, *Nucleic Acids Res*. **2009**, *37*, 5589–5601.

[30] C. G. Peng, M. J. Damha, *Nucleic Acids Res.* **2007**, *35*, 4977–4988.

[31] G. Ying, X. Lu, J. Mei, Y. Zhang, J. Chen, X. Wang, Z. Ou, Y. Yi, *Bioorg. Med. Chem.* **2019**, *27*, 3201–3207.

[32] A. Pasternak, F. J. Hernandez, L. M. Rasmussen, B. Vester, J. Wengel, *Nucleic Acids Res.* **2011**, *39*, 1155–1164.

[33] N. Borbone, M. Bucci, G. Oliviero, E. Morelli, J. Amato, V. D'Atri, S. D'Errico, V. Vellecco, G. Cirino, G. Piccialli, C. Fattorusso, M. Varra, L. Mayol, M. Persico, M. Scuotto, *J. Med. Chem.* **2012**, *55*, 10716–10728.

[34] W. Kotkowiak, J. Lisowiec-Wachnicka, J. Grynda, R. Kierzek, J. Wengel, A. Pasternak, *Mol. Ther. - Nucleic Acids* **2018**, *10*, 304–316.

[35] W. Kotkowiak, J. Wengel, C. J. Scotton, A. Pasternak, *J. Med. Chem.* **2019**, *62*, 2499–2507.

[36] A. Virgilio, L. Petraccone, M. Scuotto, V. Vellecco, M. Bucci, L. Mayol, M. Varra, V. Esposito, A. Galeone, *Chembiochem*. **2014**,*15*, 2427-2434.

[37] M. Kovacic, P. Podbevsek, H. Tateishi-Karimata, S. Takahashi, N. Sugimoto, J. Plavec, *Nucleic Acids Res.* **2020**, *48*, 3975–3986.

[38] B. Saccà, L. Lacroix, J-L. Mergny, *Nucleic Acids Res.* **2005**, *33*, 1182–1192.

[39] A. M. Varizhuk, V. B. Tsvetkov, O. N. Tatarinova, D. N. Kaluzhny, V. L. Florentiev, E. N. Timofeev, A. K. Shchyolkina, O. F. Borisova, I. P. Smirnov, S. L. Grokhovsky, A. V. Aseychev, G. E. Pozmogova, *Eur. J. Med. Chem.* **2013**, *67*, 90–97.

[40] I. Smirnov, R. H. Shafer, *Biochemistry* **2000**, *39*, 1462–1468.

[41] M. Varada, M. Aher, N. Erande, V. A. Kumar, M. Fernandes, *ACS Omega* **2020**, *5*, 498-506.

[42] L. Martino, A. Virno, A. Randazzo, A. Virgilio, V. Esposito, C. Giancola, M. Bucci, G. Cirino, L. Mayol, *Nucleic Acids Res.* **2006**, *34*, 6653–6662.

[43] C. Riccardi, A. Meyer, J.-J. Vasseur, I. Russo Krauss, L. Paduano, F. Morvan, D. Montesarchio, *Bioorg Chem.* **2020**, *94*,103379.

[44] N. A. Kolganova, V. B. Tsvetkov, I. P. Smirnov, E. N. Timofeev, *Nucleic Acid Ther.* **2019**, *29*, 208-217.

[45] (a) D. D'Alonzo, A. Guaragna, A. Van Aerschot, P. Herdewijn, G. Palumbo, *Tetrahedron Lett.* **2008**, 49, 6068-6070; (b) D. D'Alonzo, A. Van Aerschot, A. Guaragna, G. Palumbo, G. Schepers, S. Capone, J. Rozenski, P. Herdewijn, *Chem. – Eur. J.* **2009**, *15*, 10121–10131.

[46] D. D'Alonzo, A. Guaragna, Van Aerschot, P. Herdewijn, G. Palumbo, *J. Org. Chem.* **2010**, *75*, 6402–6410.

[47] D. D'Alonzo, J. Amato, G. Schepers, M. Froeyen, A. Van Aerschot, P. Herdewijn, A. Guaragna, *Angew. Chem. Int. Ed.* **2013**, *52*, 6662–6665.

[48] D. D'Alonzo, M. Froeyen, G. Schepers, G. Di Fabio, A. Van Aerschot, P. Herdewijn, G. Palumbo, A. Guaragna, *J. Org. Chem.* **2015**, *80*, 5014–5022.

[49] C. Paolella, D. D'Alonzo, G. Schepers, A. V. Aerschot, G. Di Fabio, G. Palumbo, P. Herdewijn, A. Guaragna, *Org. Biomol. Chem.* **2015**, *13*, 10041–10049.

[50] D. D'Alonzo, A. Guaragna, G. Palumbo, *Chem. Biodivers.* **2011**, *8*, 373–413.

[51] P. Herdewijn, *Chem. Biodivers.* **2010**, *7*, 1–59.

[52] P. Herdewijn, *Antiviral Res.* **2006**, *71*, 317–321.

[53] C. Hendrix, H. Rosemeyer, I. Verheggen, A. V. Aerschot, F. Seela, P. Herdewijn, *Chem. – Eur. J.* **1997**, *3*, 110–120.

[54] J. Zhou, M. Abramov, F. Liu, S. Amrane, A. Bourdoncle, P. Herdewijn, J.-L. Mergny, *Chem. – Eur. J.* **2013**, *19*, 14719–14725.

[55] H. Kang, M. H. Fisher, D. Xu, Y. J. Miyamoto, A. Marchand, A. Van Aerschot, P. Herdewijn, R. L. Juliano, *Nucleic Acids Res.* **2004**, *32*, 4411–4419.

[56] B. T. Le, S. Chen, M. Abramov, P. Herdewijn, R. N. Veedu, *Chem. Commun.* **2016**, *52*, 13467–13470.

[57] V. B. Pinheiro, A. I. Taylor, C. Cozens, M. Abramov, M. Renders, S. Zhang, J. C. Chaput, J. Wengel, S.-Y. Peak-Chew, S. H. McLaughlin, P. Herdewijn, P. Holliger *Science* **2012**, *336*, 341–344.

[58] A. I. Taylor, V. B. Pinheiro, M. J. Smola, A. S. Morgunov, S. Peak-Chew, C. Cozens, K. M. Weeks, P. Herdewijn, P. Holliger, *Nature* **2015**, *518*, 427–430.

[59] E. Eremeeva, P. Herdewijn, *Curr. Opin. Biotechnol.* **2019**, *57*, 25–33.

[60] G. Kolb, S. Reigadas, C. Boiziau, A. van Aerschot, A. Arzumanov, M. J. Gait, P. Herdewijn, J.-J. Toulmé, *Biochemistry* **2005**, *44*, 2926–2933.

[61] E. Eremeeva, A. Fikatas, L. Margamuljana, M. Abramov, D. Schols, E. Groaz, P. Herdewijn, *Nucleic Acids Res.* **2019**, *47*, 4927–4939.

[62] A. M. Varizhuk, V. B. Tsvetkov, O. N. Tatarinova, D. N. Kaluzhny, V. L. Florentiev, E. N. Timofeev, A. K. Shchyolkina, O. F. Borisova, I. P. Smirnov, S. L. Grokhovsky, A. V. Aseychev, G. E. Pozmogova, *Eur. J. Med. Chem.* **2013**, *67*, 90-97.

10.1002/chem.202001504

[63] Z. Zhou, J. Zhu, L. Zhang, Y. Du, S. Dong, E. Wang, *Anal. Chem.* **2013**, *85*, 2431−2435.
[64] I. M. Lagoja, A. Marchand, A. van Aerschot, P. Herdewijn, *Curr. Protoc. Nucleic Acid Chem.* **2003**, *14*, 1.9.1-1.9.22.
[65] L.A. Marky, K.J. Breslauer, *Biopolymers* **1987**, *26*, 1601-1620.
[66] R. De Cristoforo, E. Di Cera, *J Protein Chem*. **1991**, *10*, 455-468.
[67] A. Randazzo, G. P. Spada, M. W. da Silva, M. W. in *Quadruplex Nucleic Acids* (Eds.: J. B. Chaires, D. Graves) Topics in Current Chemistry; Springer: Berlin, Heidelberg, **2013**, pp. 67–86.
[68] J. L. Mergny, A. T. Phan, L. Lacroix, *FEBS Letters* **1998**, *435*, 74-78; M.
[69] A. M. Kopylov, T.M. Jackson, M.E. Stroupe, *Molecules* **2019**, *24*, pii. E1988.
[70] N. G. Dolinnaya, A. V. Yuminova, V. A.Spiridonova, A. M. Arutyunya, A. M. Kopylov, *J. Biomol. Struct. Dyn.* **2012**, *30*, 524-531.

10.1002/chem.202001504

WILEY-VCH

FULL PAPER

Entry for the Table of Contents

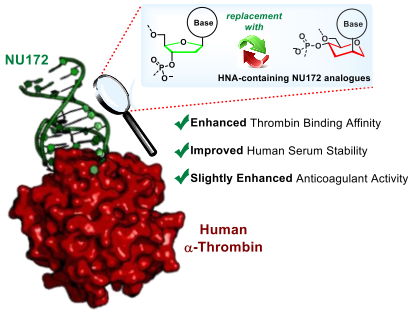

Something NU: the first SAR study of the potent anticoagulant agent NU172, following the replacement of one or more nucleotides with their unnatural counterparts belonging to the HNA (Hexitol Nucleic Acids) family, is herein reported. Compared to unmodified NU172, one HNA-containing mutant exhibited preferable physicochemical and functional properties, because of the higher binding affinity to α-thrombin, the improved stability in human serum and the slightly enhanced anticoagulant activity.